




Scalable Imaging Device Using Line Scan Camera for Use in Biometric Recognition and Medical Imaging

Michal Dvořák¹^a, Ondřej Kanich¹^b and Martin Drahanský¹^c

¹*Faculty of Information Technology, Brno University of Technology, Brno, Czech Republic
{idvorakmi, kanich, drahan}@fit.vutbr.cz*

Keywords: Imaging System, Fingerprint, Hand Geometry, Line-scan Camera, Skin Diseases

Abstract: In this paper, a novel imaging system for use in a biometric or medical application utilizing a line scan camera is being presented. The system utilizes a linear motion system to achieve a variable field of view as per operators' demands, while maintaining the high resolution per unit area. Use cases are presented using several demonstrations of possible applications. Fingerprint quality evaluation algorithms are showing applicability as a biometric-enabled system. Dermatological application is demonstrated by using the acquired images to perform a measurement of common nevi. Further uses in wound treatment and other biometrics such as hand geometry recognition and palmprint recognition are discussed.

1 INTRODUCTION

Whether the goal is to perform medical imaging for dermatology or wound care purposes, or perhaps data for biometric applications are required, there is a need to collect the images of a human body in a precise, repeatable, and high-quality manner. Despite cameras being widespread, and their parameters soaring in the last couple of years, when the application demands highly detailed images of large areas of the human body, it can be quickly discovered that even the available high-resolution cameras are insufficient. It is then necessary to either come up with a way to utilize the less detailed imagery or to find a way to generate a sufficient number of high-quality 2D sub-images that can be reconstructed into the final image. Both methods have their drawbacks. What if, however, instead of using a traditional 2D camera sensor with a fixed number of pixels per area, a sensor with variable field of view was made?

The goal of this work is to present a design and a prototype of an optical scanning device, utilizing a line scanner instead of a traditional 2D sensor. A device that can change the field of view based on the operators' needs and thus allowing for scanning body parts of various sizes without having to change the

physical configuration of the device. A device that can facilitate scanning of a finger, a hand or a whole arm without having to sacrifice an image quality.


In this paper, a possible configuration of the device is demonstrated by capturing images of human hands and acquiring a small database. This decision has been made to allow the use of biometric quality evaluation to establish the performance of the device.


1.1 Use Cases


The intended application of this device is a medical imaging in the visible, near-infrared or ultraviolet spectrum with a focus on usability in dermatology and potentially a wound treatment such as shown in (Dick et al., 2019), (Zhang et al., 2017), (Deng et al., 2017) and the technologies developed for this purpose, most notably by (Korotkov et al., 2015) and (Haeghen et al., 2000). The device was designed for tracking the change or rate of change of selected features such as various skin lesions and scar tissues.

1.2 Operation Principle

Unlike the traditional 2D CMOS or CCD sensor, where during the acquisition the whole target object is projected onto the sensor and is downloaded from

^a <https://orcid.org/0000-0003-3265-6955>

^b <https://orcid.org/0000-0003-0093-8536>

^c <https://orcid.org/0000-0002-9321-7385>

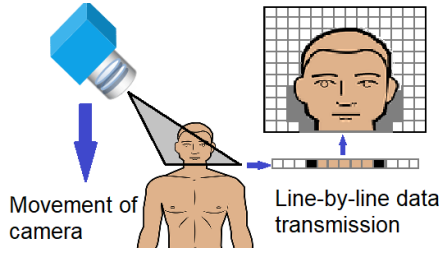


Figure 1: Line scanner principle (Fermum, 2016).

the camera after that, the proposed device utilizes a line scanner instead.

The general operating principle of line scanner can be seen in Figure 1. During the acquisition, the camera captures information regarding a line whose width w_{r1} is determined by the camera and camera lens parameters. In this paper, the axis that corresponds to the acquired line will be described as a sensor axis and the perpendicular axis will be called the movement axis.

To reconstruct the complete image of the target, either the camera or the target needs to move along the movement axis at a predefined speed v_s and the acquisition must be performed at a rate of f .

$$f = 1/\tau \quad (1)$$

$$\tau = 1/2 \cdot w_{r1}/v_s \quad (2)$$

Where f [Hz] is the rate of acquisition in lines per second. τ [s] is the period between acquisitions. w_r [mm] is the resolvable width which is required and v_s [mms⁻¹] is the speed of the system. The factor of $1/2$ is necessary to meet the Nyquist–Shannon (NS) sampling theorem (Nyquist, 1928) due to the movement of the system.

1.3 Optical Principle

Given the distance to the target object and the size of the chosen sensor, the camera lens needs to be calculated. To determine the appropriate camera lens, the required field of view fov_w needs to be considered. In this case, fov_w describes the maximum dimension (width) of the target that can be observed with chosen optics. fov_θ represents a field of view expressed as an angle.

$$fov_{w2} = 2s \cdot \tan(\theta/2) \quad (3)$$

$$fov_\theta = 2 \cdot \arctan(h/2f) \quad (4)$$

s is a distance to our target, f is the focal length of our chosen lens and h is the actual size of the sensor. The focal distance (Ray, 2004) f can be calculated using the required distance to the object, also known

as object distance g , and ratio of sensor size to target size, also known as the magnification m (Ray, 2004).

$$f = mg/(1 + m) \quad (5)$$

The size of the smallest resolvable object w_{r2} which can be scanned in the sensor axis can be determined from the resolution of used sensor r_s and the fov_2 using the following formula.

$$w_{r2} = 2 \cdot fov_{w2}/r_s \quad (6)$$

Where the factor of two ensures NS sampling theorem is met. For completeness, the following formula derived from (2) and (3) denotes the resolvability limit in the axis of the movement.

$$w_{r1} = 2 \cdot v_s/f \quad (7)$$

For the traditional 2D sensor, the field of view in both dimensions would need to be considered, however, for line scanner, the field of view of the movement axis is defined purely by the physical dimension of the scanner in the axis of the movement.

For finite image, the field of view of the image in the axis of the movement fov_{w1} can be simply defined as a function of time t .

$$fov_{w1} = v_s \cdot t \quad (8)$$

1.4 Requirements for Biomedical and Biometric Applications

The most known biometric systems are touch-based fingerprint sensors used in mobile phones or laptops. Other devices use hand geometry, finger vein or palm vein for the recognition process (Debiasi et al., 2018). One thing these devices often have in common is the necessity to touch the sensing area. Especially now, the hygienic demands dictate that the devices used by multiple people need to be cleaned and disinfected at regular intervals. This paper offers an approach where no optical element needs to be touched.

The human hand contains much information that can be used for biometric recognition (Drahanský & Kanich, 2019). The focus of this article is to analyze fingerprint and hand geometry characteristics with limited discussion concerning the feasibility of palmprint and vein extraction.

The spatial resolution used for fingerprint recognition is typically 500 dpi (dots per inch) for the commercial devices but can be performed with images with resolution as low as 300 dpi (Drahanský et al., 2018).

Customarily, the hand is placed onto a designated surface to limit the user’s movement. High contrast images are desirable for valleys and ridges to be easily distinguishable.

For the hand geometry, the resolution requirements are lower than for fingerprints. For successful hand shape extraction, the scanned area needs to be large enough for the whole hand up to the wrist to be visible.

For biomedical purposes, the device needs to be calibrated to give the device an ability to measure the size of the studied objects. The external light source and repeatable scanning allows the comparison of the studied objects and evaluate the rate of change in size, colour or structure (Dick et al., 2019).

2 DEVICE DESIGN

In this part, the general requirements and consequent design of the scanner will be discussed along with a list of components that have been used for the prototype described in this paper.

2.1 Optical Design

Following parameters are defined.

1. The spatial resolution of the image is to be at least 350 dpi.
2. The scanned area is to be at least 400×180 mm.

The first requirement allows to resolve objects of approximately 0.145 mm. It ensures that both the biometric applications and the calibrated measurement for a medical imaging application can be performed. Both requirements are used to define linear scanner itself, as the minimum resolution can be derived from them in the following manner.

$$R_{min} = 350 \cdot (400/25.4) \approx 5,512 \quad (9)$$

Based on this requirement, a line scanner *raL6144-16gm Basler* with the resolution of 6,144 px has been chosen as suitable.

Formula (5) can be used to find a suitable camera lens. The object distance of the device is 535 mm, as further discussed in subsection 2.2. Given the dimensions of the chosen sensor and the target area dimensions, the magnification needs to be at least 0.096 to guarantee the 350 dpi requirement. Using the formula (5), the focal length can be calculated to be 47 mm. 50 mm camera lens has been used due to its availability. This guarantees a resolution of 350 dpi

for the area of 417.1 mm. Camera lens *AF Nikkor 50mm f/1.8D* has been used in the device. The *Chromasens Corona II type C* with LED-control unit *XLC4-1* has been used for illumination.

2.2 Mechanical and Electrical Design

The main computing unit is a single board computer (SBC) *Raspberry Pi 3*. It has been decided that the movement subsystem will be controlled by a separate microcontroller (MCU) *Arduino Uno*.

Figure 2 illustrates how are the individual components connected. The functionality and purposes of individual subsystems are further described in subsection 2.3.

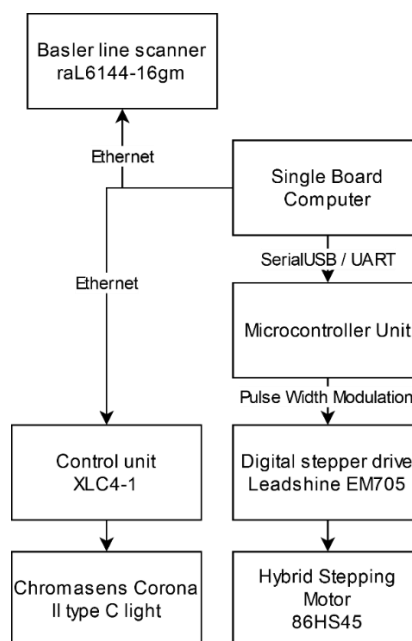


Figure 2: Functional diagram of the device, illustrating individual subsystem and communication interfaces.

For power, the device utilized three *Manson NP-9615 DC* regulated power supplies to generate 48 V, 24 V, 12 V and 5 V for voltage branches. The summary of electrical requirements for the used components can be found in Table 1.

The conversion of rotational movement of the stepper motor into the linear motion necessary for the scanning has been realized using a linear motion system with a threaded rod *NL208TR-1200* made by T.E.A. Technik (T.E.A Technik s.r.o., 2020). This system, considering the method of scanning, allows for objects up to 120×43 cm in size to be scanned while maintaining the 350 dpi spatial resolution or in other words, it functions as approximately 100 Mpx industrial-grade camera.

Table 1: Electrical parameters of components.

Component	Voltage [V]	Maximum current [A]
raL6144-16gm	12	0.375
XLC4-1	24	3
CORONA II	24	1.8
EM705	48	-
86HS45	48	4.2
RPI3	5	2.5
Arduino UNO r3	12	-

The Figure 3 represents a front view of the hardware setup in schematics form, along with the physical dimensions in mm. The dimension 345 mm represents the maximum range the scanner can move and, therefore, also the maximum dimension of the resulting image along this axis. During the database collection, the users approached the device from the front, placed the hand onto the *Hand placement platform* and the scanner performed a complete image acquisition by moving from left to right.

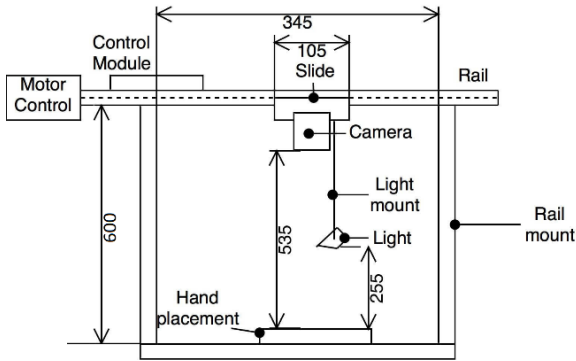


Figure 3: Construction design of the scanner.

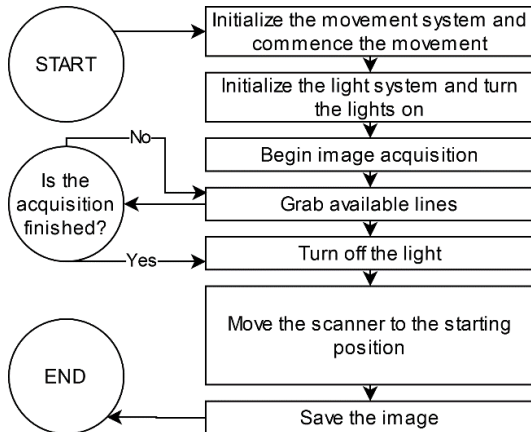


Figure 4: The function calls sequence during the scanning process.

2.3 Control System

The SBC either directly or indirectly controlled each part of the device. Figure 4 shows the control structure and the way in which the modules are sequentially called.

2.3.1 Light Control

The SBC was communicating with the *XLC4-1* unit using Telnet interface over the ethernet. Series of simple commands provided by the unit's documentation were used to set the intensity of the light and to turn the light module on and off. Commands to monitor the status of the unit and the module were also utilized.

2.3.2 Movement Control

The MCU has performed movement control to avoid unexpected interruptions of the SBC. Using the USART interface, a command from SBC is sent to MCU that contains a piece of information about requested direction and distance to be travelled. MCU parses this command and using the HW timer and counter, it generates a pulse sequence with a frequency of 62.5 kHz for the appropriate number of ticks.

EM705 stepper driver is set for micro-stepping at 12,800 steps per revolution. This, combined with the physical property of *NL208TR-1200* which performs a lateral movement of 4 mm per one revolution, gives us a precise function that defines the distance travelled d in millimetres as a function of time t in seconds in the following manner.

$$d(t) = 4 \cdot (62,500 \cdot t) / 12,800 \quad (10)$$

The prototype for the database collection used a scanning time of 10,000 ms (10 s), covering 195.31 mm of distance.

2.3.3 Line Scanner Control

The line scanner is controlled by SBC using the GigE interface and Basler API. The script developed for this purpose handles proper initialization, data grabbing and image construction. All triggering and frame grabbing is performed using software scripts.

The prototype due to standard dimensions of the target performs acquisition of 5,120 lines at a rate of 500 lines per second. Considering the movement speed of the linear movement system, the chosen rates cause a line width to be 0.039 mm. Due to the apparent difference of the vertical pixel size from the horizontal pixel size, the image is upscalded by a factor of two in the x-axis prior being saved.

3 DATA COLLECTION

The choice has been made to use a visible light source for image acquisition. For the application, it was chosen to test fingerprint recognition which requires very precise images of the ridges and recognition based on hand geometry which can use both sides of the hand.

3.1 Database Collection

Per the design decisions outlined in previous sections of this paper, the device generates images with the resolution of $6,144 \times 5,120$ px that are upscaled to $12,288 \times 5,120$ px for easier visual inspection. The scanned area is 417.1×195.3 mm which corresponds to the spatial resolution of 375 dpi in the scanner axis and 666 dpi in the movement axis. In Figure 5, two sample images are presented.

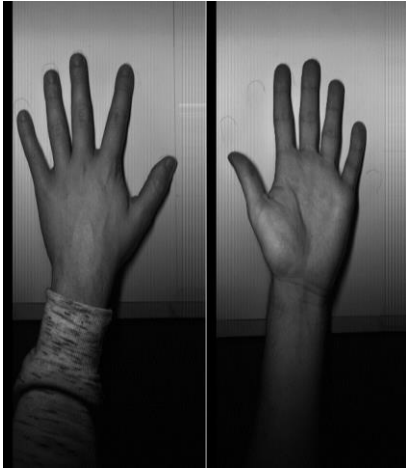


Figure 5: Example of dorsal hand surface image (left) and palmar surface image (right).

The image collection was done without adhering to any specific condition, in an ordinary room with daylight and artificial light present. Volunteers came into the room and one or both of their hands were acquired from palmar and/or dorsal side.

Overall, 145 images were acquired. These contained 77 hands from the volunteers in the 20-30 age group, mixed gender. 56 of these images are from the palmar side, remaining 89 from the dorsal side.

3.2 Images Applications

It is essential to remind the reader that the device was developed primarily as a scanning method and that the biometric quality evaluation serves primarily to gauge the image quality.

3.2.1 Biometric Recognition – Fingerprints

Due to large scanned area, the preprocessing aims to localize and extract fingerprints, these subimages are then enhanced as the algorithms for the fingerprint evaluation, generally expecting binarized or at least normalized data.

Hand extraction started with coarse image alteration. In this step, a rectangle of 7,800 px to 4,300 px is isolated from position $x = 4,500$ px and $y = 225$ px. Cropped images contain only the hand and a part of the wrist. Images were rotated so that fingers pointed upwards and background was thresholded away.

Using convolution-based localization algorithms, the probable position of fingers was determined. Figure 6 shows result of the finger localization. After getting the finger images, histogram equalization and local thresholding methods are used to normalize the image and to increase the contrast of the ridges. Result can be seen in the Figure 7.

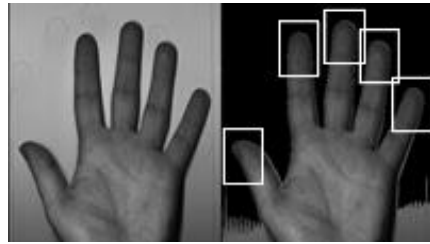


Figure 6: Input image (left) and isolated fingers (right).



Figure 7: Example of two processed fingerprints.

280 images containing 230 fingerprints were acquired from the images. The fingerprints were then evaluated using VeriFinger (version 10) (Neurotechnology, 2018) and FiQiVi (Dejmal, 2019). The median VeriFinger quality was 32 (maximum 60, minimum 10), FiQiVi showed a median of 38 (maximum 57 and minimum 19). For biometric recognition the VeriFinger developer Neurotechnology recommends the quality of at least 40 for identification and 30 for verification. This has also been experimentally verified by (Alsmirat et al., 2018).

While the quality of the fingerprints may seem low, it is an impressive score. Firstly, the device to facilitate the large area acquisition used a 375 dpi resolution, which is lower than it is usual for fingerprint sensors. Secondly, unlike the almost absolute majority of sensors, this device does not use a scanning surface against which the finger is to be pressed. Thus, it reduces the available scanning area due to the finger geometry, as it is not pressed against a glass surface, as well as decreases the contrast due to the absence of total internal reflection. This concept can be seen in (Maltoni et al., 2009) Thirdly, this evaluation contained also thumbs which were usually acquired at an angle. Lastly, only basic image pre-processing was done with no fingerprint enhancement algorithms being used. Therefore, the fact that despite all the disadvantages, the device still manages to meet the fingerprint biometry baseline is a relatively strong proof of its viability.

3.2.2 Biomedical Applications

The device is mainly intended to be used for monitoring hand diseases and disorders, such as eczema, as well as various skin growths, such as nevus, to monitor their size and area. In the previous section, it was shown that the device is able to distinguish ridges that have a width from 0.2 to 0.5 mm (Drahanský et al., 2011). Based on fixed optics and calibrated system, precise measurements can be performed.

Figure 8 (top) provides a detailed image of nevi on one user's hand. Due to the system being calibrated, we can determine that a bounding box of 34×29 px and 24×19 px that can be used to surround the nevi corresponds to size of 1.23×1.13 mm and 0.87×0.74 mm respectively. The analysis of the size of the nevi can be immediately performed as well as saved and compared during subsequent scanning for any change. The same process can be used to observe the rate or any changes in the wound healing process. This can be seen in Figure 8 (bottom) were mutilated

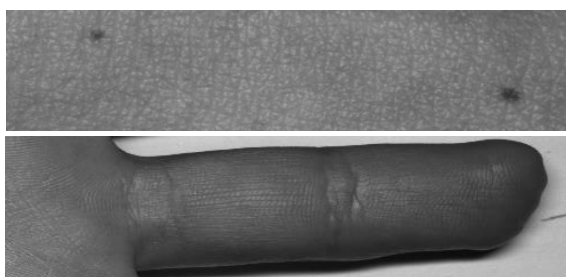


Figure 8: Detail of nevi (top). Regenerated friction ridges on the fingertip (bottom).

finger is present but the current images clearly show that the friction ridges are restored on the remainder of the finger.

3.2.3 Biometric Recognition – Hand Geometry

The images collected by the scanner are of sufficient quality to perform recognition based on hand geometry if other biometrics are unavailable, for example, due to injuries such as a burn or skin diseases.

As the acquisition process is calibrated and the images can be used to perform measurements of the target object, absolute measurements may be used as a feature set for the recognition algorithms, such as described by (Pititeeraphab & Pintavirooj, 2018) and (Wirayuda et al, 2013) or relative measurement, as described by (Siswanto et al, 2013).

Majority of algorithms perform segmentation and work with a binarized image of the hand, which these images can also be converted to. The feature set can then be constructed from such features as outlined in the Figure 9. Given the knowledge that pixel's height corresponds to 0.039 mm and the pixel's width corresponds to 0.036 mm. Using this information, any selected length of the image may be recalculated into a real-world dimension.

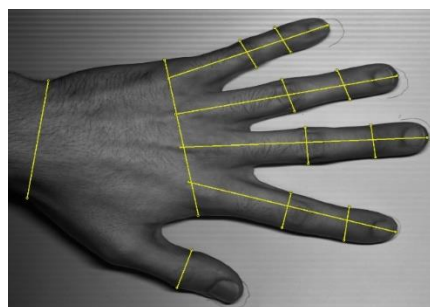


Figure 9: Proposed hand geometry features.

3.2.4 Biometric Recognition – Other Characteristics

Due to the image size and resolution, additional biometric features can be extracted. Figure 10 shows the enhanced image of the palmar side of the hand indicating a multitude of data for possible biometric (e.g. palmprint recognition). In this paper, visible light source has been used, however, should the other wavelength be used, other data may be acquired. The use of near-infra lighting near the 850 nm wavelength would allow for an observation of veins such as (Huang et al., 2018), again usable for biometric or medical purposes.

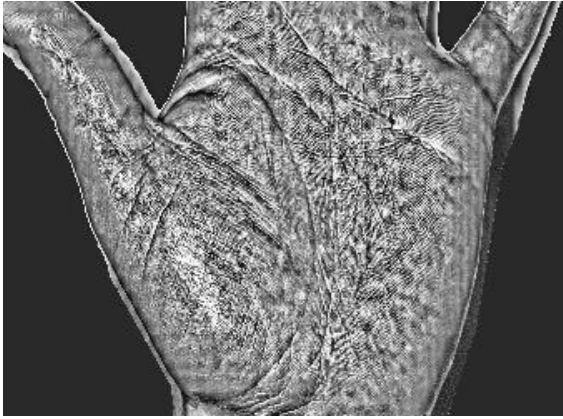


Figure 10: Example of enhanced image of the palmprint.

3.3 Discussion of the Results

The presented results and images serve as a demonstration of the viability of line scan cameras for biomedical and biometric application. The ability to perform scans of various lengths gives this system flexibility the devices with traditional 2D sensors lack. It can also achieve very good precision on the whole scanned area. There are some disadvantages as well. Scanned user has to remain calm during the scanning process and line cameras can be expensive.

3.3.1 The Device as a Biometric System

In the article, fingerprint and hand geometry recognition has been discussed and its efficiency evaluated. It can be concluded that while the device would need to be modified for it to be a more effective biometric system, the values from commercial and academic quality assessment algorithms indicate that even as it is, the device could be used for biometric application. This, more than anything, speaks of the image quality received from the device and proves its efficacy in scanning live objects which, to the knowledge of the authors, has not been widely explored for line scan cameras.

Applicability of the hand geometry recognition and palmprint recognition has been discussed, while the usability of the palmprint is implied by the fact that the images may be used for fingerprint recognition. There is, to the knowledge of the authors, no available tool to measure the image quality for the hand geometry recognition. Therefore, only relevant research into existing literature has been done.

3.3.2 The Device as a Biomedical System

Based on the available literature, the skin images of sufficient quality may be used to analyze various skin

growths. It has been demonstrated, both in the design of the device and in the final images, that the skin images offer sufficient quality to perform imaging and extract a precise measurement of the various skin objects. Should the scanning be repeated, a change in time can be observed.

4 CONCLUSIONS

This paper introduces an optical scanning device using line scan camera, linear movement system, light unit, single board computer and microcontroller capable of producing images of the variable field of view without having to make concessions to the quality due to its mechanical properties.

The laboratory prototype of the device was constructed and pilot data collection consisting of 145 human hands, of which 56 was palmar side up, was conducted. The function and the performance of the device have been tested to determine its efficiency as a biometric and biomedical system. The first test was focused on the possibility of using acquired images for fingerprint recognition. Overall, 280 fingerprint images were extracted from the database and analyzed using two fingerprint quality assessment systems. The image quality of the majority of the extracted fingerprints has been determined to be sufficient for fingerprint verification and identification.

Dorsal and palmar images of hand were examined for the usage in hand geometry recognition as well as performing measurements of various skin features usable for biomedical application. These measurements are suitable for monitoring nevi, skin diseases analysis and a rate of change in the wound healing process. Based on the analysis, it was decided that the detail of the images is sufficient.

To sum it up, the device can obtain high-quality images. The examined object did not have to touch the sensing area. Size of the images is limited by the defined width of the camera, but scalable in the movement axis, limited only by the linear motion system's properties. Within the limits of the motion system, the change of the image size due to the movement axis does not require any physical changes to the device and can be changed programmatically by the operator.

For further research, the device could be enlarged and used as a full-frontal body scanner. Optimization of the biometric extraction process would lead to higher performance rate for the biometric applications.

ACKNOWLEDGEMENTS

This research has been realized under the support of the following grants: Technology Agency of the Czech Republic from the ÉTA programme "Survey and education of citizens of the Czech Republic in the field of biometrics – TL02000134", "Reliable, Secure, and Efficient Computer Systems" – internal Brno University of Technology project FIT-S-20-6427.

REFERENCES

- Alsmirat, M. A., Al-Alem, F., Al-Ayyoub, M., Jararweh, Y., Gupta, B., 2018. *Impact of digital fingerprint image quality on the fingerprint recognition accuracy*. Multimedia Tools and Applications, 78(3), 3649-3688. <https://doi.org/10.1007/s11042-017-5537-5>
- Debiasi, L., Kauba, C., Prommegger, B., Uhl, A., 2018. *Near-Infrared Illumination Add-On for Mobile Hand-Vein Acquisition*. 2018 IEEE 9th International Conference on Biometrics Theory, Applications and Systems (BTAS). <https://doi.org/10.1109/BTAS.2018.8698575>
- Dejmal, D., 2019. *Analýza systémů pro měření kvality otisku prstů* [Bachelor's thesis, Brno University of Technology]. <https://www.fit.vut.cz/study/thesis-file/19344/19344.pdf>
- Deng, Z., Fan, H., Xie, F., Cui, Y., Liu, J., 2017. *Segmentation of dermoscopy images based on fully convolutional neural network*. 2017 IEEE International Conference on Image Processing (ICIP). <https://doi.org/10.1109/icip.2017.8296578>
- Dick, V., Sinz, C., Mittlböck, M., Kittler, H., Tschandl, P., 2019. *Accuracy of Computer-Aided Diagnosis of Melanoma*. JAMA Dermatology, 155(11), 1291. <https://doi.org/10.1001/jamadermatol.2019.1375>
- Drahanský, M. (Ed.), 2018. *Hand-Based Biometrics: Methods and technology*. IET, ISBN 978-1-78561-224-4.
- Drahanský, M., Kanich, O., 2019. Influence of Skin Diseases on Fingerprints. In Nait-Ali, A. (Ed.), *Biometrics under Biomedical Considerations*. Springer. <https://doi.org/10.1007/978-981-13-1144-4>
- Drahanský, M., Orság, F., Dvořák, R., Hájek, J., Váňa, J., Herman, D., Kněžík, J., Marvan, A., Lodrová, D., Doležel, M., Hanáček, P., Mráček, Š., Stružka, J., 2011. *Biometrie*. Cumpster Press s.r.o. ISBN 978-80-254-8979-6.
- Fermum, L., 2016 (n.d.). *Line scan camera basics*. Retrieved November 05, 2020, from <https://www.vision-doctor.com/en/line-scan-cameras/line-scan-camera-basics.html>
- Haeghen, Y., Naeyaert, J., Lemahieu, I., Philips, W., 2000. *An imaging system with calibrated color image acquisition for use in dermatology*. IEEE Transactions on Medical Imaging, 19(7), 722-730. <https://doi.org/10.1109/42.875195>
- Huang, Q., Hu, K., Zhou, P., Luo, Y., Wu, L., 2018. *Design of Finger Vein Capturing Device Based on ARM and CMOS Array*. 2018 2nd IEEE Advanced Information Management, Communicates, Electronic and Automation Control Conference (IMCEC). <https://doi.org/10.1109/imcec.2018.8469403>
- Korotkov, K., Quintana, J., Puig, S., Malveyh, J., Garcia, R., 2015. *A New Total Body Scanning System for Automatic Change Detection in Multiple Pigmented Skin Lesions*. IEEE Transactions on Medical Imaging, 34(1), 317-338. <https://doi.org/10.1109/tmi.2014.2357715>
- Maltoni, D., Maio, D., Jain, A. K., Prabhakar, S., 2009. *Handbook of Fingerprint Recognition*. Springer, Second Edition, ISBN 978-1-84882-253-5.
- Neurotechnology, 2018. *MegaMatcher 10.0, VeriFinger 10.0, VeriLook 10.0, VeriEye 10.0 and VeriSpeak 10.0 SDK – Developer's Guide*. Neurotechnology, Version: 10.0.0.0.
- Nyquist, H., 1928. *Certain Topics in Telegraph Transmission Theory*. Transactions of the American Institute of Electrical Engineers, 47(2), 617-644. <https://doi.org/10.1109/t-aiee.1928.5055024>
- Pititeeraphab, Y., Pintavirooj, C., 2018. *Identity Verification Using Geometry of Human hands*. 2018 11th Biomedical Engineering International Conference (BMEiCON). <https://doi.org/10.1109/bmeicon.2018.8609986>
- Ray, S. F., 2004. *Applied photographic optics: Lenses and optical systems for photography, film, video, and electronic imaging*. Oxford: Focal Press, Third edition. ISBN 978-0-24051-540-3.
- Siswanto, A., Tarigan, P., Fahmi, F., 2013. *Design of contactless hand biometric system with relative geometric parameters*. 2013 3rd International Conference on Instrumentation, Communications, Information Technology and Biomedical Engineering (ICICI-BME). <https://doi.org/10.1109/icicibme.2013.6698492>
- T.E.A. TECHNIK s.r.o., 2020. *Lineární osa se šroubem NL*. T.E.A. TECHNIK s.r.o. Retrieved November 04, 2020, from <https://www.teatechnik.cz/linearni-osa-sroubem-nl/>
- Wirayuda, T. A., Kuswanto, D. H., Adhi, H. A., Dayawati, R. N., 2013. *Implementation of feature extraction based hand geometry in biometric identification system*. 2013 International Conference of Information and Communication Technology (ICoICT). <https://doi.org/10.1109/icoict.2013.6574583>
- Zhang, X., Wang, S., Liu, J., Tao, C., 2017. *Computer-aided diagnosis of four common cutaneous diseases using deep learning algorithm*. 2017 IEEE International Conference on Bioinformatics and Biomedicine (BIBM). <https://doi.org/10.1109/bibm.2017.8217850>